

Vibrational spectra of an RDX film over an aluminum substrate from molecular dynamics simulations and density functional theory

Julibeth M. Martínez de la Hoz · Perla B. Balbuena

Received: 25 July 2012 / Accepted: 1 October 2012 / Published online: 20 October 2012
© Springer-Verlag Berlin Heidelberg 2012

Abstract We report calculated vibrational spectra in the range of 0–3,500 cm^{-1} of RDX (hexahydro-1,3,5-trinitro-1,3,5-triazine) molecules adsorbed on a model aluminum surface. A molecular film was modeled using two approaches: (1) density functional theory (DFT) was used to optimize a single RDX molecule interacting with its periodic images, and (2) a group of nine molecules extracted from the crystal structure was deposited on the surface and interacted with its periodic images via molecular dynamics (MD) simulations. In both cases, the molecule was initialized in the AAA conformer geometry having the three nitro groups in axial positions, and kept that conformation in the DFT examination, but some molecules were found to change to the AAE conformer (two nitro groups in axial and one in equatorial position) in the MD analysis. The vibrational spectra obtained from both methods are similar to each other, except in the regions where collective RDX intermolecular interactions (captured by MD simulations) are important, and compare fairly well with experimental findings.

Keywords Density functional theory · Molecular dynamics simulations · RDX film · Explosive materials · Thin films

Introduction

The vibrational properties of explosive solids are of great interest not only because they allow the elucidation of

mechanisms leading to detonation initiation [1] but also because of the possibility of detection of specific substances [2, 3]. Each material has characteristic vibrational modes in the terahertz (THz) and infrared (IR) range (1–430 THz) that can be used to identify the presence of explosives. Moreover, recently there has been increased interest in the use of Terahertz spectroscopy [3] because it permits the observation of features related to the crystal structure in the range of 1–4 THz involving intra and intermolecular modes, which are relevant in real composite materials due to their complexity. Therefore, the identification of the IR and THz vibrational signatures of high explosive materials would constitute a significant contribution to the understanding and characterization of these materials.

RDX (hexahydro-1,3,5-trinitro-1,3,5-triazine) is an important energetic compound. It belongs to the class of explosives nitroamines and it is used widely in military and industrial applications, i.e., automobile air bags and rocket propellants [4]. An important theoretical tool available for this analysis is offered by a combination of DFT and MD methods. Computational efforts have focused on the IR spectrum of a few conformers using density functional theory (DFT) methods [5, 6]. Also, the IR spectrum of the RDX crystal has been calculated using molecular dynamics (MD) simulations [1]. Other previously calculated IR spectra of RDX have shown good agreement with experimental results [6, 7].

Experimentally, the THz spectrum of the RDX has been obtained using disordered polycrystalline pellets in most cases, which makes it hard to characterize individual modes due to the inhomogeneous broadening of the local vibrations. However, a recent experimental work [8] showed that this problem could be addressed by forming instead a polycrystalline film of RDX on a metal surface and analyzing the

J. M. Martínez de la Hoz · P. B. Balbuena (✉)
Department of Chemical Engineering,
and Materials Science and Engineering Program,
Texas A&M University,
College Station, TX 77843, USA
e-mail: balbuena@tamu.edu

system using the terahertz (THz) time domain spectroscopy technique. The interesting THz spectrum is found to be in the range from 0.5 to 3.5 THz, which can be complemented by adding the IR vibrational spectrum to fully characterize the RDX modes. In previous work [9, 10], we used DFT calculations to evaluate the vibrational spectra of RDX monomers in gas phase: AAE (having two NO₂ groups in axial positions and one in equatorial position) and AAA (with the three NO₂ groups in nearly axial positions) as well as the effect of intermolecular interactions in the dimer and tetramer. In gas phase, our calculations at B3LYP/6-311 G (d,p) level indicated that AAE-RDX is 0.55 kcal mol⁻¹ more stable than the AAA conformer [9]. Rice et al. [5] reported 0.19 kcal mol⁻¹ calculated at B3LYP/6-31 G(d) [11] and 0.64 kcal mol⁻¹ at B3LYP/6-311+G(d,p), in reasonable agreement with our results. Various RDX crystalline forms exist: α , β , δ , γ , and ϵ , [12], of which α is the most stable at room temperature [13] where crystal packing is stabilized by CH \cdots O intermolecular interactions between a methylene hydrogen of one molecule and oxygen atoms belonging to nitro groups of a neighbor molecule [14].

Surfaces and defects can influence adsorption and reaction of energetic molecules as reported extensively by Kuklja et al. [15]. In order to determine the effect of a substrate on the molecular conformation, we also analyzed the RDX/Al₁₆ complex, where we found that the most favorable RDX molecular geometry is closer to that of the AAA conformation. However, comparison of the spectra of the gas phase AAA monomer, the Al₁₆ surface, and that of the complex reveals significant differences. In-plane modes of Al₁₆ are shifted to higher frequencies in the complex, and several new coupled modes (Al₁₆-RDX) appear between 200 and 400 cm⁻¹ in the complex. Other differences were revealed in the mid-IR region of the spectra, where the modes of the molecule attached to the model aluminum surface were red-shifted with respect to those in the free

molecule due to interactions of the NO₂ group with the metal atoms.

Due to the significance of molecular modeling methods for elucidation of properties in complex systems [16–19] that are sometimes difficult to evaluate experimentally, here we refine our previous calculations by incorporating some of the possible collective effects when a film of RDX molecules interacts with a metal surface. We calculated the IR spectrum of a layer of RDX molecules over a model Al (111) surface using two different approaches. In the first, we used DFT methods to evaluate the adsorption and vibrational spectrum of one RDX molecule on a (3 \times 3) Al surface represented by a two-layer slab. Using periodic boundary conditions, the single molecule interacts with its images emulating a model RDX monolayer adsorbed over the aluminum slab. In the second approach, we used MD simulations to investigate a system consisting of an actual layer of nine RDX molecules taken from the crystal structure and placed over a two-layer slab with a 7 \times 7 periodic surface of aluminum. The spectra obtained are then studied, and the respective modes corresponding to each frequency are characterized. This information is expected to help in the understanding of the vibrational modes of a RDX thin film adsorbed on an aluminum surface, therefore providing further information for sensor devices.

Methods

The initial RDX molecular geometry and the unit cell of the RDX crystal were taken from the Cambridge crystallographic database [14]. For the DFT calculation, fixed cell geometry optimization and harmonic normal modes analysis were performed with the CASTEP simulation software [20] using the exchange-correlation functional Perdew–Burke–Ernzerhof (GGA-PBE) [21], a cutoff energy of 220 eV and a 3 \times 3 \times 1 k-points Monkhorst–Pack

Fig. 1 Final configuration of the system consisting of one molecule of RDX (hexahydro-1,3,5-trinitro-1,3,5-triazine) over two layers of a 3 \times 3 slab of Al(111) after density functional theory (DFT) optimization. **a** Lateral view of the unit cell. **b** Top view of four unit cells. *Magenta* Aluminum, *red* oxygen, *blue* nitrogen, *grey* carbon, *white* hydrogen

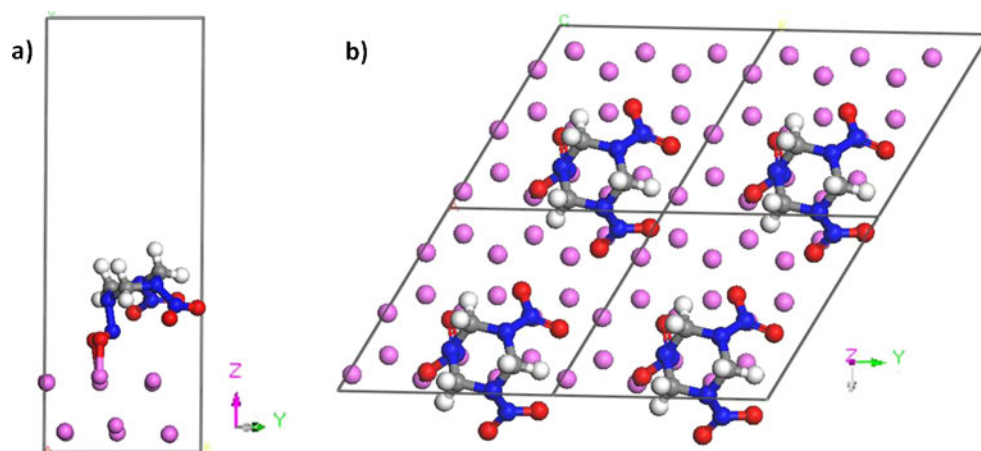
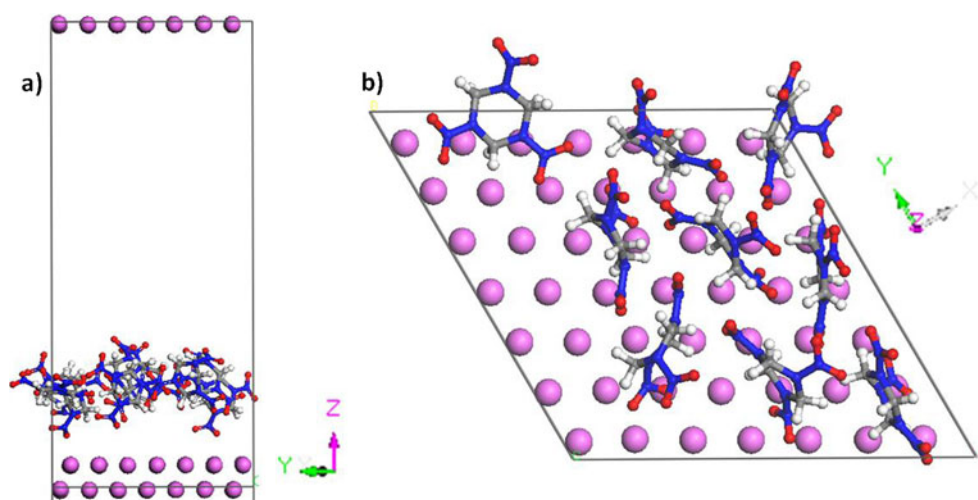


Fig. 2 Final configuration of the system consisting of nine molecules of RDX and two layers of a 7×7 slab of Al(111) after 1 ns of molecular dynamics (MD) simulation at 10 K and 1 atm. **a** Lateral view of the unit cell. **b** Top view of the unit cell. Magenta Aluminum, red oxygen, blue nitrogen, grey carbon, white hydrogen



[22] mesh sampling in the surface Brillouin zone. The convergence criterion used for the electronic self-consistent iteration was 5×10^{-7} eV/atom and the vibrational frequencies and eigenvectors at the selected set of q-vectors in the Brillouin zone were calculated using the finite displacement method [23].

The model used for the DFT calculations consisted of one RDX molecule, placed on a two-layer 3×3 slab of aluminum, using the closed packed plane (111) of the face-centered cubic (fcc) structure. Periodic boundary conditions were applied in the x , y and z directions, and a vacuum space of about 20 Å was applied in the surface normal direction to avoid interactions between the slab and its periodic image. The initial configuration of the RDX molecule onto the aluminum surface was that of the AAA conformer, in which all the nitro groups are located in axial positions. This initial configuration was chosen for the RDX molecule based on previous theoretical work in which the AAA was found as the most stable configuration for the RDX molecule adsorbed on a layer of aluminum [9]. It is important to mention that the crystalline form associated with this conformer, known as the β form, has been confirmed recently and fully analyzed experimentally [24, 25]. The single AAA molecule was optimized previous to the calculation with the aluminum layer using the VASP simulation package [26–30], with the GGA-PBE functional, a cutoff energy of 400 eV and a $9 \times 9 \times 1$ k-points Monkhorst-Pack mesh sampling. In this case the convergence criterion used for the electronic self-consistent iteration was 1×10^{-8} eV.

MD simulations were carried out using the DLPOLY-2 simulation package [31]. The isothermal-isobaric NPT ensemble [32] was used at 10 K and 1 atm, the temperature and pressure being controlled through the Berendsen's thermostat and barostat [32] using the same value of 0.4 ps as relaxation time both for the thermostat and barostat, respectively. The equilibration length was determined by the decrease in fluctuations of total energy of the system

as a function of time. When the difference between the instantaneous total energy and its average was less than $\pm 10^{-4}$ eV/atom, the system was considered at equilibrium. To model the interaction among the aluminum atoms on the metal slab, the Sutton-Chen potential with published parameters [33] was used. RDX molecules were modeled using the force field of Boyd et al. [7], and the interaction between RDX and the aluminum slab was represented by a Lennard-Jones potential using the mixing values $\sigma_{ij} = \frac{\sigma_{ii} + \sigma_{jj}}{2}$ and $\epsilon = \sqrt{\epsilon_{ii} \cdot \epsilon_{jj}}$. The values for the pure elements were taken from published data [34].

The simulated RDX crystal consisted of $3 \times 3 \times 3$ unit cells (216 molecules); within a periodic orthorhombic super cell of $38.7 \times 33.5 \times 32.1$ Å³ which was relaxed for 150 ps until equilibrium was reached. Then, a layer of this relaxed crystal (9 molecules of RDX) was placed onto a two layer 7×7 slab of Al (111). In this case, the system also reached equilibrium after 150 ps. However, the total simulation length was extended to 1 ns to assure total relaxation of the equilibrated system. The final configuration of the system (shown in Fig. 2), was then used to calculate the IR

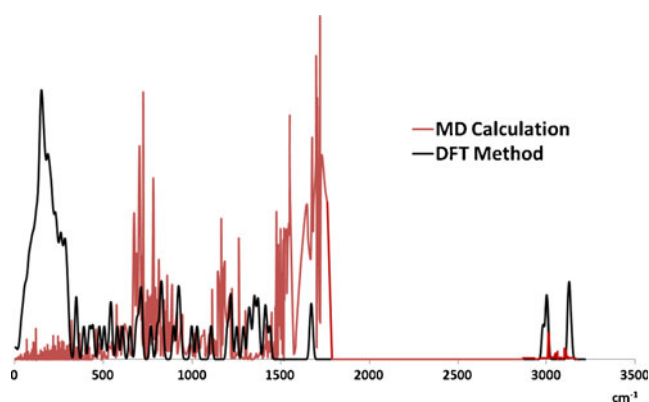


Fig. 3 Comparison among the spectrum calculated from the system shown in Fig. 1 using a DFT method and the spectrum calculated from the system shown in Fig. 2 using a MD method

spectrum using the time correlation function method implemented in the DISCOVER simulation software [35]. In this approach, the IR lineshape is calculated by Fourier transformation of the autocorrelation function of dipole moments for a given system [36, 37]. The ab-initio based force field COMPASS [38] (condensed-phase optimized molecular potentials for atomistic simulation studies) was used since it has shown to be capable of making accurate predictions of

structural and vibrational properties for a broad range of compounds, both in isolation and condensed phases [39–41].

Results and discussion

The configuration of the systems after DFT optimization and MD equilibration is shown in Figs. 1 and 2, respectively.

Table 1 Main vibrational modes calculated for the RDX (hexahydro-1,3,5-trinitro-1,3,5-triazine)–Al (111) system using a density functional theory (DFT) and a molecular dynamics (MD) method

DFT method		MD calculation	
Frequency (cm ⁻¹)	Mode	Frequency (cm ⁻¹)	Mode
145.35	Al in-plane vibrations	67.7	Al in-plane vibrations
168.23	Al in-plane vibrations	119.2	Al in-plane vibrations
213.99	NO ₂ twisting+Al out of plane vibrations	217.2	NO ₂ twisting+Al out of plane vibrations
236.88	Al in-plane vibrations	244.0	Al in-plane vibrations
261.51	Al in-plane vibrations+ring twisting	320.0	NC ₂ Rocking
340.72	Ring twisting	458.0	CH ₂ Rocking+CN ₂ scissoring
354.80	NC ₂ Rocking	575.0	NC ₂ Twisting+NC ₂ asymmetrical stretching
418.26	CH ₂ Rocking	671.0	NO ₂ Twisting+NC ₂ asymmetrical stretching
419.99	NO ₂ Rocking+CH ₂ rocking	701.0	NO ₂ Wagging
437.52	CH ₂ Rocking+CN ₂ scissoring	723.0	NO ₂ Wagging
500.88	CH ₂ Rocking+CH ₂ wagging	780.0	NO ₂ Wagging
536.09	NO ₂ Scissoring+NC ₂ scissoring+CH ₂ Rocking	811.0	NC ₂ Symmetrical stretching
571.3	NC ₂ Twisting+NC ₂ asymmetrical stretching	858.0	NC ₂ Symmetrical stretching
573.09	NC ₂ Twisting+NC ₂ asymmetrical stretching	885.0	CH ₂ Rocking+NO ₂ Wagging
578.33	CN ₂ Scissoring	915.0	CH ₂ Rocking+CN ₂ asymmetrical stretching
641.7	NO ₂ Scissoring+NC ₂ scissoring	1111.0	CN ₂ Asymmetrical stretching
705.1	NO ₂ Wagging	1163.0	CH ₂ Rocking+NC ₂ asymmetrical stretching
761.4	CH ₂ Rocking+NC ₂ scissoring	1262.0	CH ₂ Twisting
819.5	CH ₂ Rocking+NC ₂ symmetrical stretching+NO ₂ asymmetrical stretching	1475.0	CH ₂ Scissoring
888.1	CH ₂ Rocking+NO ₂ wagging	1550.0	CH ₂ Scissoring
918.02	CH ₂ Rocking+CN ₂ asymmetrical stretching	1670.0	NO ₂ Asymmetrical stretching
990.18	CN ₂ Rocking+CH ₂ rocking	1698.0	NO ₂ Asymmetrical stretching
991.94	CN ₂ Rocking+CH ₂ rocking	1720.0	NO ₂ Asymmetrical stretching
1021.9	CH ₂ Rocking+CH ₂ twisting	3012.0	CH ₂ Asymmetrical stretching
1101.1	CN ₂ Asymmetrical stretching	3049.0	CH ₂ Asymmetrical stretching
1213.71	NC ₂ Asymmetrical stretching	3100.0	CH ₂ Asymmetrical stretching
1226.03	CH ₂ Rocking+NC ₂ scissoring		
1285.9	CH ₂ Wagging+NO ₂ symmetrical stretching		
1315.8	CH ₂ Wagging		
1347.5	CH ₂ Twisting		
1409.08	CH ₂ Scissoring		
1424.9	CH ₂ Scissoring		
1669.6	NO ₂ Asymmetrical stretching		
2977.3	CH ₂ Asymmetrical stretching		
2996.7	CH ₂ Asymmetrical stretching		
3121.6	CH ₂ Asymmetrical stretching		

After DFT optimization of the system as shown in Fig. 1, the molecule of RDX seems to retain its AAA geometry in which all the nitro groups are in axial positions. The bond length among each of the two oxygen atoms bonded to the aluminum surface and the surface is around 1.8 Å.

On the other hand, the geometry of the RDX molecules shown in Fig. 2 varies from molecule to molecule. Some RDX molecules in this system display structures closer to the AAA conformer, while others are closer to the AAE. The average distance from the closest oxygen atoms to the aluminum surface is 2.7 Å. This may be a consequence of the lower stability of the AAA with respect to the AAE conformer [25].

The spectra calculated using DFT and MD methods were compared (Fig. 3). Although the relative intensities vary on the different regions of the spectra, the peaks are located around the same frequencies (approximately 0–1730 and 2970–3120 cm^{-1}). The modes corresponding to the peaks shown in each spectrum are summarized in Table 1.

In the region from 0 to 400 cm^{-1} the modes corresponding to Al in-plane vibrations, Al out-of-plane vibrations, NO_2 twisting and NC_2 rocking are observed in both spectra. Additionally, ring twisting is seen at 261.5 and 340.7 cm^{-1} in the DFT spectrum. From 400 to 950 cm^{-1} the modes observed in both spectra are CH_2 rocking, CN_2 scissoring, NC_2 symmetrical and asymmetrical stretching, NC_2 twisting and NO_2 wagging. Also, CH_2 wagging, NO_2 rocking, NO_2 scissoring and NO_2 asymmetrical stretching are seen in this region of the DFT spectrum. NO_2 twisting appears at 671 cm^{-1} in the MD spectrum. From 950 to 1790 cm^{-1} CH_2 rocking, CH_2 scissoring, CH_2 twisting, CN_2 asymmetrical stretching, NC_2 asymmetrical stretching and NO_2 asymmetrical stretching were found in both spectra. In addition, CN_2 rocking, NC_2 scissoring, CH_2 wagging and NO_2 symmetrical stretching can be observed in this region of the DFT spectrum. No peaks are observed in the DFT spectrum between 1424.9 and 1669.6 cm^{-1} while some may be seen at 1475 and 1550 cm^{-1} in the MD spectrum.

However they both correspond to CH_2 scissoring, which is the same mode that corresponds to the peak at 1424.9 cm^{-1} in the DFT spectrum. Finally, all the peaks observed in both spectra after 2900 cm^{-1} correspond to CH_2 asymmetrical stretching.

These spectra compared very well to the ones calculated in our previous work [9]. For example, in the case of an AAA-RDX monomer, peaks between 750 and 1050 cm^{-1} are related to CH_2 rocking and NC_2 stretching; peaks around 1200–1550 cm^{-1} correspond to CH_2 wagging, scissoring and twisting vibrations and groups around 1680 cm^{-1} relate to NO_2 asymmetrical stretching [9]. These same modes are found around the same frequencies in the spectra shown in Fig. 3. Furthermore, the spectrum found using one layer of a 4×4 surface of aluminum (111) and a monomer of RDX without applying periodic boundary conditions in our previous work [9], does not display any peaks in the region from 1482 to 1603 cm^{-1} . Something similar is observed in the DFT spectrum of Fig. 3. This uses only one molecule of RDX and does not display any peaks between 1424.9 and 1669.6 cm^{-1} . However, the MD spectrum (Fig. 3) shows some peaks between these frequencies that correspond to the mode reflected at 1424.9 cm^{-1} in the DFT spectrum, which may suggest an amplification in the region where the modes are observed due to the interaction among RDX molecules. This same phenomenon is observed in the regions 701–811 cm^{-1} , 811–915 cm^{-1} and 1111–1262 cm^{-1} of the MD spectrum with respect to DFT.

It is also useful to compare the spectra obtained in this work with the experimental spectrum found in a previous work by different authors at 7 K using a layer of RDX molecules over an aluminum plate [8]. Since the spectrum obtained by the DFT method is very similar to the spectrum obtained by the MD method in the region from 0 to 120 cm^{-1} (Fig. 4a), the former is used to compare to the experimental spectrum in this region (Fig. 4b). As in our previous work [9], the peaks observed are around 36, 49, 54, 62, 71, 82, 98, 104 and 115 cm^{-1} , corresponding to Al in-

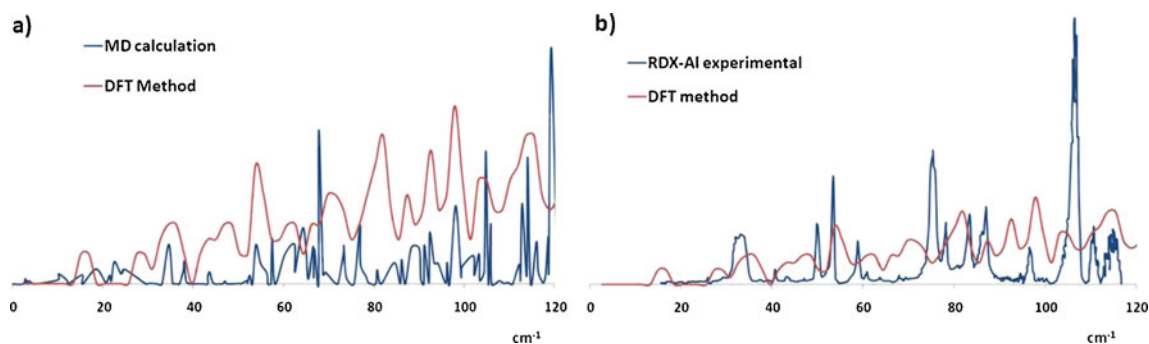


Fig. 4 Spectra showing frequencies from 0 from 120 cm^{-1} . **a** Overlap of the spectra obtained by MD and DFT methods. **b** Overlap of the spectrum obtained experimentally [8] and that

obtained by DFT methods in this work. The vertical scales are different in both graphs to be able to fit the experimental intensities in **b**

plane and out-of-plane vibrations, NO₂ rocking and NO₂ libration.

Recent work has shown that the THz spectra obtained from molecules adsorbed on different metal substrates are independent of the nature of the substrate [42]. Although our results find the presence of in-plane and out-plane vibrations of the Al surface, they are not in contradiction with the experimental observation because it is possible that various metal surfaces (Cu, Au, Al surfaces reported in the particular experiment) [42] may yield similar vibrational modes in the THz region, thus affecting the spectral features of the adsorbed molecule similarly.

Conclusions

The vibrational spectrum corresponding to a molecule of RDX over two layers of a 3×3 slab of aluminum (111) was obtained by periodic DFT methods, along with the spectrum for nine molecules of RDX over two layers of a 7×7 slab of Al (111) evaluated by MD methods. The modes corresponding to the vibrational frequencies found in each spectrum are assigned. Comparison of the two calculated spectra reveals the presence of the same modes located at very similar frequencies. However, the spectrum obtained by MD methods reflects an enhancement of the region where the observed modes are due to interactions among RDX molecules. Good agreement is observed between these spectra and those calculated in a previous work for a monomer of RDX, a molecule of RDX over a 4×4 slab of aluminum and an experimental spectrum reported previously in the literature.

Acknowledgments We gratefully acknowledge financial support from the US Army Research Office and the US Defense Threat Reduction Agency (DTRA). Computational resources from TAMU Supercomputer Facility, University of Texas TACC, and National Energy Research Scientific Computing Center (NERSC) are also acknowledged.

References

- Boyd SG, Boyd KJ (2008) *J Chem Phys* 129:134502–134511
- Steinfeld JI, Wormhoudt J (1998) *Annu Rev Phys Chem* 49:203–232
- Leahy-Hoppa M, Fitch M, Osiander R (2009) *Anal Bioanal Chem* 395:247–257
- Moore DS (2004) *Rev Sci Instrum* 75:2499–2512
- Rice BM, Chabalowski CF (1997) *J Phys Chem A* 101:8720–8726
- Allis DG, Zeitler JA, Taday PF, Korter TM (2008) *Chem Phys Lett* 463:84–89
- Boyd S, Gravelle M, Politzer P (2006) *J Chem Phys* 124:104508–104510
- Melinger JS, Laman N, Grischkowsky D (2008) *Appl Phys Lett* 93:011102–011103
- Guadarrama-Pérez C, Martínez de La Hoz JM, Balbuena PB (2010) *J Phys Chem A* 114:2284–2292
- Guadarrama-Pérez C, de la Hoz JMM, Balbuena PB (2010) *J Phys Chem A* 114:7815–7815
- Vladimiroff T, Rice BM (2002) *J Phys Chem A* 106:10437–10443
- Millar DIA, Oswald IDH, Francis DJ, Marshall WG, Pulham CR, Cumming AS (2009) *ChemComm* 473:562–564
- McCrone WC (2002) *Anal Chem* 22:954–955
- Hakey P, Ouellette W, Zubieta J, Korter T (2008) *Acta Crystallogr Sect E* 64:o1428
- Sharia O, Kuklja MM (2012) *J Am Chem Soc* 134:11815–11820
- Murray JS, Redfern PC, Seminario JM, Politzer P (1990) *J Phys Chem* 94:2320–2323
- Politzer P, Seminario JM (1993) *Chem Phys Lett* 216:348–352
- Murray JS, Seminario JM, Politzer P (1994) *Int J Quantum Chem* 49:575–579
- Politzer P, Ma YG (2004) *Int J Quantum Chem* 100:733–739
- Segall MD et al (2002) *J Phys Condens Matter* 14:2717
- Perdew JP, Burke K, Ernzerhof M (1996) *Phys Rev Lett* 77:3865–3868
- Monkhorst HJ, Pack JD (1976) *Phys Rev B* 13:5188
- Montanari B, Harrison NM (2002) *Chem Phys Lett* 364:528–534
- Millar DIA, Oswald IDH, Francis DJ, Marshall WG, Pulham CR, Cumming AS (2009) *Chem Commun* 5:562–564
- Goldberg IG, Swift JA (2012) *Cryst Growth Des* 12:1040–1045
- Kresse G, Furthmüller J (1996) *Phys Rev B* 54:11169
- Kresse G, Furthmüller J (1996) *Comput Mater Sci* 6:15–50
- Kresse G, Hafner J (1993) *Phys Rev B* 48:13115
- Kresse G, Hafner J (1993) *Phys Rev B* 47:558
- Kresse G, Hafner J (1994) *Phys Rev B* 49:14251
- Smith W, Forester TR (1996) *J Mol Graph* 14:136–141
- Berendsen HJC, Postma JPM, van Gunsteren WF, DiNola A, Haak JR (1984) *J Chem Phys* 81:3684–3690
- Raffi-Tabar H, Sulton AP (1991) *Philos Mag Lett* 63:217–224
- Mayo SL, Olafson BD, Goddard WA (1990) *J Phys Chem* 94:8897–8909
- Accelrys (2008) *Materials Studio 4.4*, <http://accelrys.com>
- Gordon RG (1965) *J Chem Phys* 42:3658–3665
- Gordon RG (1968) *Adv Mag Reson* 3:1
- Sun H (1998) *J Phys Chem B* 102:7338–7364
- Sun H, Rigby D (1997) *Spectrochim Acta A Mol Biomol Spectrosc* 53:1301–1323
- Rigby D, Sun H, Eichinger BE (1997) *Polym Int* 44:311–330
- Spyriouni T, Vergelati C (2001) *Macromolecules* 34:5306–5316
- Harsha SS, Melinger JS, Qadri SB, Grischkowsky D (2012) *J Appl Phys* 111:023105